

Fast radio bursts from axion stars moving through pulsar magnetospheres

James H. Buckley,^{*} P. S. Bhupal Dev,[†] Francesc Ferrer,[‡] and Fa Peng Huang[§]

*Department of Physics and McDonnell Center for the Space Sciences,
Washington University, St. Louis, MO 63130, USA*

We study the radio signals generated when an axion star enters the magnetosphere of a neutron star. As the axion star moves through the resonant region where the plasma-induced photon mass becomes equal to the axion mass, the axions can efficiently convert into photons, giving rise to an intense, transient radio signal. We show that a dense axion star with a mass $\sim 10^{-13} M_\odot$ composed of $\sim 10 \mu\text{eV}$ axions can account for most of the mysterious fast radio bursts.

Weakly coupled pseudoscalar particles such as axions, that arise from a solution to the strong CP-problem [1], or more generic axion-like particles (ALPs) predicted by string theory [2], are promising dark matter (DM) candidates and may contribute significantly to the energy density of the Universe [3]. In recent years, an increased interest on axion DM has bolstered a broad experimental program [4], often based on the Primakoff process [5], whereby axions transform into photons in external magnetic fields and vice versa.

Low mass axions or ALPs that contribute appreciably to the DM must have extremely high occupation numbers, and can be modeled by a classical field condensate. Such large number density in astrophysical environments enables to probe their existence indirectly through the detection of low energy photons. For μeV -scale axions consistent with the observed DM density, the emitted photons have frequencies in the range probed by radio telescopes. Along these lines, signals resulting from the axion decay to two photons [6], or from resonant axion-photon conversion [7–9] have been recently explored.

If the Peccei-Quinn (PQ) symmetry [1] is broken after inflation, the axionic DM distribution is expected to be highly inhomogeneous, leading to the formation of axion miniclusters as soon as the Universe enters the matter-domination regime [10], which in turn may lead to the formation of dense boson stars [11] that could make part of the DM [12]. Such boson stars are called axion stars, when the kinetic pressure is balanced by self-gravity, or axitons, when stabilized by self-interactions (see Ref. [13] for a recent review). Gravitational microlensing could potentially constrain the fraction of DM in collapsed structures [14], but typical axion star signals fall in the femtolensing regime which is not robustly constrained [15]. Although their presence may be unveiled in future by observations of highly magnified stars [16], it is important to look for other experimental probes.

Such dense clumps of axion DM can lead to enhanced radio signals, which might explain the mysterious observation of Fast Radio Bursts (FRBs) [17, 18]. For instance, the oscillating axion configuration of a dilute axion star hitting the atmosphere of a neutron star could induce dipolar radiation of the dense electrons in the atmo-

sphere [19] or neutrons in the interior [20], and generate a powerful radio signal. However, as noted in Ref. [21], the dilute star will be tidally disrupted well before reaching the surface of the neutron star. Moreover, the plasma mass of a photon radiated at the surface of the neutron star is much larger than the frequency of the dipole radiation. Hence, medium effects would greatly suppress the signal.

Even the optimistic scenario of a dense axion star directly hitting the NS surface would lead to, at most, a μJy radio signal [22], whereas FRBs range from $\mathcal{O}(0.1)$ to $\mathcal{O}(100)$ Jy. Their large dispersion measure suggests that the FRBs are of extragalactic origin, $0.1 \lesssim z \lesssim 2.2$, which means that the total energy released is about $\mathcal{O}(10^{38} - 10^{40})$ erg, and their observed millisecond duration requires that the radiated power reaches $10^{41} - 10^{43} \text{ erg} \cdot \text{s}^{-1}$. Although their origin and physical nature are still obscure [23], the fact that the energy released by FRBs is about $10^{-13} M_\odot$, which is the typical axion star mass, and that their frequency (several hundred MHz to several GHz) coincides with that expected from μeV axion particles, motivates us to further explore whether the axion-FRB connection can be made viable in a neutron star environment and tested with future data.¹

In this paper, we propose a new explanation for FRBs based on the resonant axion-photon conversion that takes place when a dense axion star passes through the *resonant region* in the magnetosphere of a neutron star, as shown in Fig. 1. We will mainly focus on non-repeating FRBs in this work, since repeating FRBs may correspond to a different source class [26]. So far, more than 60 non-repeating FRBs have been observed [27, 28] mainly by Parkes, ASKAP, and UTMOST. Our explanation of the non-repeating FRB signals roughly from 800 MHz to 1.4 GHz involves dense stars made of axions with mass about $10 \mu\text{eV}$.

The properties of an axion star depend on its mass M_a , axion mass m_a and decay constant f_a . Dilute axion stars

¹ See Refs. [24, 25] for alternative proposals not involving neutron star.

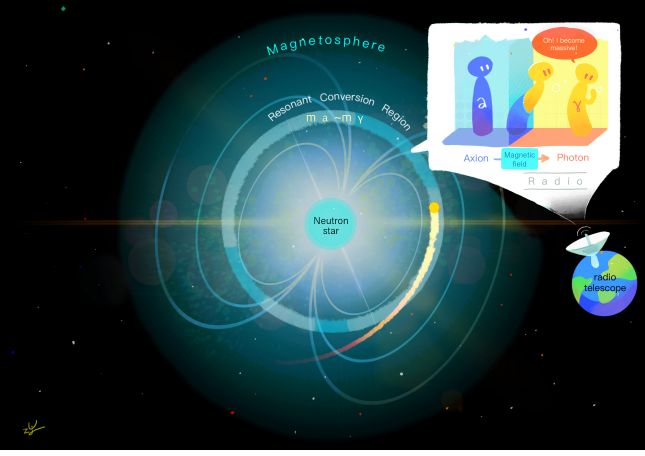


FIG. 1. Schematic diagram of the proposed FRB signal from dense axion star. When a dense axion star passes through the resonant conversion region in the magnetosphere of neutron star (where the effective photon mass equals the axion mass), powerful transient radio signals can be produced in the strong external magnetic field through the Primakoff process.

have a radius [29]

$$R_a^{\text{dilute}} \sim \frac{1}{G_N M_a m_a^2} \cong (270 \text{ km}) \left(\frac{10 \text{ } \mu\text{eV}}{m_a} \right)^2 \left(\frac{10^{-12} M_\odot}{M_a} \right). \quad (1)$$

Hence, the typical radius of a dilute axion star is $\mathcal{O}(100)$ km for the star mass range $M_a \sim 10^{-14} - 10^{-12} M_\odot$. A dense star branch was first proposed in Ref. [30]. Nevertheless, it was pointed out in Ref. [31] that axion field values reach $\gtrsim \mathcal{O}(1)$ in the core, thus making the axions relativistic and rendering the analysis in Ref. [30] inconsistent (see also Refs. [32–34]). Since gravity is negligible inside such dense stars, their profiles can instead be found as solutions of a Sine-Gordon type equation leading to their natural identification with oscillons. In contrast to the natural expectation that localized, finite energy configurations of the axion field decay within $\tau \sim 1/m_a$, oscillons can last $\mathcal{O}(100-1000)$ oscillations [35], before disappearing into a burst of relativistic axions [10]. For a QCD axion, these timescales still fall short of being of cosmological relevance. Nevertheless, flatter potentials at large field values in well motivated ALP models have been shown to feature much longer-lived oscillons, $\tau > (10^{8-9})/m_a$, and for plateau-like potentials only lower bounds on their lifetime are known [36]. Stable dense profiles are also possible when $f_a \gtrsim 0.1 M_{\text{Pl}}$ [37]. On the other hand, axion stars could have been created much after matter domination via parametric amplification of axion fluctuations even if the PQ symmetry is broken before inflation [36, 38]. Given that oscillons are attractor solutions, it cannot be excluded that dense ax-

ion configurations are being generated and are present in astrophysical settings such as pulsars [39]. In this work, we assume that dense axion stars with a mass around $10^{-13} M_\odot$ can survive to the present, and have a chance to encounter a neutron star. For dense axion stars, the radius can be approximated as [30]

$$R_a^{\text{dense}} \sim (0.47 \text{ m}) \sqrt{g_{a\gamma\gamma} \times 10^{13} \text{ GeV} \frac{10 \text{ } \mu\text{eV}}{m_a}} \times \left(\frac{M_a}{10^{-13} M_\odot} \right)^{0.3}, \quad (2)$$

with $g_{a\gamma\gamma}$ being the axion-photon coupling.

Tidal effects become important when the distance of the axion star to the neutron star approaches the Roche limit:

$$r_t = R_a \left(\frac{2M_{\text{NS}}}{M_a} \right)^{1/3}, \quad (3)$$

where M_{NS} is the neutron star mass. A gravitationally bound object approaching a star closer than this radius will be disrupted by tidal effects [21, 24]. A 100 km dilute axion star will be destroyed at $r_t \sim 10^6$ km, long before it enters the magnetosphere. Tidal disruption may quickly rip the dilute axion star apart, producing a stream of axion debris that would then be swallowed by the neutron star. It is conceivable that the subsequent interaction of the tidal debris with the neutron star could lead to multiple radio signals, similar to the repeating FRBs [40–42], and this possibility deserves further investigation.

For a dense axion star, however, the radius is smaller than a meter and the Roche limit is about 10 km. Thus, a dense axion star can reach the resonant conversion region. Tidal forces will certainly stretch the axion star in the radial direction and compress it in the transverse direction. Since the resonant conversion region is located over a hundred Schwarzschild radii from the neutron star, we can use Newtonian gravity to estimate the tidal deformation:

$$\frac{\delta R_a}{R_a} = \frac{9M_{\text{NS}}}{8\pi\rho_{\text{AS}}r^3}, \quad (4)$$

where ρ_{AS} is the axion star density and r is its distance from the neutron star. For a typical dense axion star with $M_a \sim 10^{-13} M_\odot$, the tidal deformation is negligible, $\mathcal{O}(10^{-3})$.

When a dense axion star enters the magnetosphere, axions convert to radio signals through the axion-photon interaction term

$$\mathcal{L} = -\frac{g_{a\gamma\gamma}}{4} a F^{\mu\nu} \tilde{F}_{\mu\nu} = g_{a\gamma\gamma} a \vec{E} \cdot \vec{B}, \quad (5)$$

where a is the axion field, $F^{\mu\nu}$ the electromagnetic field strength, and $\tilde{F}^{\mu\nu}$ its dual. For $m_a \sim 10 \text{ } \mu\text{eV}$, the coupling is constrained to be $g_{a\gamma\gamma} \leq 10^{-13} \text{ GeV}^{-1}$ [43, 44]. Neutron star magnetospheres, featuring the strongest

magnetic fields known in the Universe, provide one of the best environments for axion-photon conversion. Due to the extremely small coupling $g_{a\gamma\gamma}$, however, the conversion probability is generally expected to be small. On the other hand, the conversion can be significantly enhanced in the resonant conversion region of the magnetosphere. Indeed, the photon acquires a mass due to the plasma effects in the magnetosphere [45]:

$$m_\gamma(r) \simeq \omega_p = \sqrt{\frac{e^2 n_e}{m_e}} = \sqrt{\frac{n_e}{7.3 \times 10^8 \text{ cm}^{-3}}} \mu\text{eV}, \quad (6)$$

where $n_e(r)$ is the local electron density at a distance r from the neutron star center. For simplicity, we use the Goldreich-Julian distribution [46]:

$$n_e(r) = 7 \times 10^{-2} \frac{1}{P} \frac{B(r)}{1 \text{ G}} \text{ cm}^{-3}, \quad (7)$$

where P is the rotation period of the neutron star. For the magnetic field $B(r)$, we take the dipole approximation:

$$B(r) = B_0 \left(\frac{r_{\text{NS}}}{r} \right)^3, \quad (8)$$

with B_0 being the magnetic field strength at the neutron star surface, which can reach 10^{15} G for a magnetar [47]. The scale of magnetosphere is $\mathcal{O}(100) r_{\text{NS}} \sim 1000$ km.

Note that QED vacuum polarization effects can also contribute to the photon mass [48] $m_\gamma^2 = \omega_p^2 - m_{\text{QED}}^2$, with $m_{\text{QED}}^2 = \frac{7e^2}{180\pi^2} \omega^2 \frac{B^2}{B_c^2}$ and $B_c = m_e^2/e \approx 4.4 \times 10^{13}$ G. However, comparing the two contributions,

$$\frac{\omega_p^2}{m_{\text{QED}}^2} \sim 5 \times 10^8 \left(\frac{\mu\text{eV}}{\omega} \right)^2 \frac{10^{12} \text{ G}}{B} \frac{1 \text{ s}}{P}, \quad (9)$$

we see that the QED mass term becomes negligible in our case with typical axion energy $\omega \sim 10 \mu\text{eV}$ [8].

In the resonant conversion region, the photon effectively has almost the same mass as the axion due to plasma effects:

$$\omega^2 = k_a^2 + m_a^2 \approx m_\gamma^2(r_c), \quad (10)$$

where ω is the axion-photon oscillation frequency. The mass degeneracy leads to maximal mixing and greatly enhances the conversion probability. The critical radius r_c for the resonant conversion region is obtained by enforcing the maximal mixing condition Eq. (10):

$$\left(\frac{r_{\text{NS}}}{r_c} \right)^3 \sim \left(\frac{m_a}{\mu\text{eV}} \right)^2 \frac{10^{10} \text{ G}}{B_0} \frac{P}{1 \text{ s}}. \quad (11)$$

When the dense axion star approaches r_c , resonant axion-photon conversion can occur. For most neutron star environments, the resonant conversions are

non-adiabatic [8], with the conversion rate obtained as $P_{a \rightarrow \gamma} \approx 2\pi\beta$ with

$$\beta = \frac{(g_{a\gamma\gamma} \omega B_0)^2 / 2\bar{k}}{\left| d\omega_p^2 / dr \right|} \Big|_{r=r_c}. \quad (12)$$

Here, $\bar{k} \equiv \sqrt{\omega^2 - (m_a^2 + \omega_p^2)/2}$ is the axion momentum in the diagonalized basis of the mixing equations. From Eqs. (6)-(11), we can derive

$$\frac{d\omega_p^2}{dr} \Big|_{r=r_c} = \frac{3\omega_p^2}{r} \Big|_{r=r_c}. \quad (13)$$

We note that for typical parameters, close to the neutron star surface $r < r_c$, the effective photon mass is larger than the axion mass, and the emission of a photon is kinematically suppressed, impacting the viability of the mechanisms proposed in Refs. [19, 22].

As a dense axion star moves through the resonant region, the conversion power is $\dot{W} = P_{a \rightarrow \gamma} dM_a/dt$ with $dM_a/dt \sim \pi R_a^2 \rho_A v_c$ and $\rho_A = M_a/(4\pi R_a^3/3)$. Thus, we obtain the power:

$$\dot{W} \sim \left(\frac{M_a}{10^{-13} M_\odot} \right) (10^7 \times P_{a \rightarrow \gamma}) (10^{44} \text{ GeV} \cdot \text{s}^{-1}). \quad (14)$$

For the benchmark values $B_0 = 10^{14}$ G, $m_a = 10 \mu\text{eV}$, $g_{a\gamma\gamma} = 10^{-13} \text{ GeV}^{-1}$, conversion in a typical $1.4 M_\odot$ pulsar rotating with $P = 0.1$ s occurs with $P_{a \rightarrow \gamma} \approx 2 \times 10^{-5}$ in the resonant region. Hence, a $10^{-13} M_\odot$ dense axion star can naturally account for the typical output associated to FRBs, $\dot{W} \sim 10^{44} \text{ GeV} \cdot \text{s}^{-1}$. The trajectory of a dense axion star moving roughly parallel to the resonant region is schematically shown in Fig. 1. Upon entering, the axion star moves in the resonant region for about 10 km (several milliseconds) until it leaves the region or evaporates.

To compare with the current FRB data [27, 28], we use the convention:

$$\frac{E_{\text{FRB}}}{\text{J}} = \frac{F_{\text{obs}}}{\text{Jy} \cdot \text{ms}} \frac{\Delta B}{\text{Hz}} \left(\frac{d}{\text{m}} \right)^2 \times 10^{-29} (1+z), \quad (15)$$

where E_{FRB} is the FRB energy (10^{30} to 10^{33} J), d is the source distance (from several hundred Mpc to several Gpc), and z is the redshift. ΔB is chosen as the bandwidth of the radio telescope in current experiments [27, 28]. The fluence F_{obs} is the density flux $\mathcal{S} \sim \dot{W}/(4\pi d^2 \Delta B)$ integrated over time.

For our benchmark values we can naturally explain most of the observed FRBs as shown in Fig. 2. The orange line in Fig. 2 depicts the upper limit for $M_a = 10^{-13} M_\odot$ with $\Delta B = 340$ MHz, and the events below this line can be accounted for. The dashed orange line represents the upper limit for $M_a = 10^{-12} M_\odot$ and the same bandwidth, while we used $M_a = 10^{-13} M_\odot$ and

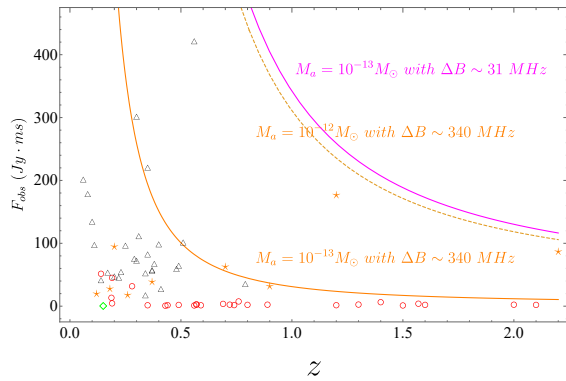


FIG. 2. Upper limit on the fluence as a function of redshift z . The solid orange line depicts the upper limit for $M_a = 10^{-13} M_\odot$ with bandwidth $\Delta B = 340$ MHz. Similarly, the dashed orange and solid magenta lines are the upper limits for $(M_a, \Delta B) = (10^{-12} M_\odot, 340 \text{ MHz})$ and $(10^{-13} M_\odot, 31 \text{ MHz})$, respectively. The red circles, black triangles, green diamonds and orange stars show the 27 non-repeating FRBs observed by Parkes ($\Delta B \sim 338.381$ MHz), 28 events from ASKAP ($\Delta B \sim 336$ MHz), 1 event from Arecibo ($\Delta B \sim 322.6$ MHz) and 9 events from UTMOST ($\Delta B \sim 31.25$ MHz), respectively [28].

$\Delta B = 31$ MHz for the magenta line. The red circles, black triangles, green diamonds and orange stars represent the 27 non-repeating FRBs observed by Parkes ($\Delta B \sim 338.381$ MHz), 28 events from ASKAP ($\Delta B \sim 336$ MHz), 1 event from Arecibo ($\Delta B \sim 322.6$ MHz) and 9 events from UTMOST ($\Delta B \sim 31.25$ MHz) [28], respectively. Most events lie below the solid orange curve, except a few events which can only be explained by a heavier axion star, as shown by the dashed orange curve. For a smaller bandwidth $\Delta B = 31$ MHz, even $M_a = 10^{-13} M_\odot$ could explain all the events by this scenario, as shown by the magenta curve.² Thus, a dense axion star with mass $\sim 10^{-13} M_\odot$, consistent with theoretical expectations [13], can explain the radiated energy of most of the observed FRB events. Those events in Fig. 2 that do not saturate this limit can be due to an axion star with a different mass or to the particular astrophysical environment. For instance, the conversion probability is determined by the neutron star properties, like the magnetic field distribution and size of the neutron star, which could in principle broaden the spectrum of axion star masses from what is considered in Fig. 2.

An FRB emitted with a frequency $\nu_0 = m_a/2\pi = 2.42 \text{ GHz}(m_a/10 \mu\text{eV})$ in the axion rest frame will be observed at a lower frequency by the time it reaches a

radio telescope on Earth mainly due to the cosmological redshift:

$$\nu = \frac{\nu_0}{1+z}. \quad (16)$$

Given the different cosmological redshifts measured for different FRB events, for a $10 \mu\text{eV}$ axion, the observed frequency ranges from 700 MHz to 2.1 GHz. Thus, we can explain most of the observed FRB events which fall in this frequency range.

We stress that our aim is to explain the broad features of FRBs, but there are a number of complicated astrophysical effects that are likely important in describing their details. The magnetosphere geometry (e.g., the position of gaps and the neutral sheet) has a significant impact on the observed signals. Moreover, there are likely to be significant feedback effects in the conversion region. As the axion star moves through the field and plasma comprising the magnetosphere, it may exert radiation pressure on the surrounding plasma. Other factors can also affect the variation of signal strengths and duration. For example, for a fixed axion mass, a larger pulsar period means a smaller r_c , and hence larger $B(r_c)$ which leads to a larger conversion probability.

The existing observational data on the degree of polarization of non-repeating FRBs are limited and inconclusive. Only 9 events have polarimetric data available [49], and the picture that emerges is unclear: some events appear to be completely unpolarized, some show only circular polarization, some show only linear polarization, and others show both [49]. Several factors can influence the specific polarization expected in our scenario. First of all, the photons produced in the magnetosphere due to axion conversion might have different polarizations depending on the local environment or viewing geometry. Moreover, additional axion-photon conversions can take place during the propagation of the FRB pulse through the intergalactic magnetic field. Each conversion is expected to generate some degree of circular polarization regardless of the initial polarization at the source, depending on the properties of the cosmological magnetic field [50]. Given these uncertainties and the lack of sufficient polarimetric data, a detailed analysis of the polarization signal in our scenario is beyond the scope of the current paper, but it is certainly worth exploring in the future whether this could be used to distinguish our model from other explanations of the FRB events.

Furthermore, the axion star and the pulsar could potentially form a binary system via e.g. three-body interactions. In this case, the orbiting axion star could pass through the pulsar magnetosphere several times to produce repeating FRBs [40–42]. A larger mass would be critical for the axion stars to survive multiple transits of the resonant conversion region. We leave the details of this mechanism for future work.

The smallest flux density that can be detected by a

² Here we only list the non-repeating FRBs with frequencies favored by the $10 \mu\text{eV}$ axion. We do not include other non-repeating FRBs with frequencies lower than 800 MHz, like the events from CHIME and Pushchino [28], which may be better explained by a lighter axion or by other sources.

radio telescope can be written as:

$$\mathcal{S}_{\min} \approx 0.09 \text{ Jy} \left(\frac{1 \text{ MHz}}{\Delta B} \right)^{1/2} \left(\frac{1 \text{ ms}}{t_{\text{obs}}} \right)^{1/2} \left(\frac{10^3 \text{ m}^2/\text{K}}{A_{\text{eff}}/T_{\text{sys}}} \right)^{1/2}, \quad (17)$$

where t_{obs} is the observation time and $A_{\text{eff}}/T_{\text{sys}}$ is the effective area to system temperature ratio. For example, the SKA Phase 1 [51] with $A_{\text{eff}}/T_{\text{sys}} = 2.7 \times 10^3 \text{ m}^2/\text{K}$, assuming $\Delta B = 1 \text{ MeV}$ and $t_{\text{obs}} = 40 \text{ ms}$, can detect a radio signal if $\mathcal{S} > \mathcal{S}_{\min} \sim 5 \times 10^{-3} \text{ Jy}$ within the frequency range 0.45 to 13 GHz. The sensitivity is expected to increase by more than an order of magnitude in Phase 2 of SKA, which will enhance its ability to detect even weaker FRBs.

The event rate can be estimated as

$$N/\text{year} \approx \sigma v_0 n_{\text{AS}} n_{\text{NS}} f_{\text{NS}} V, \quad (18)$$

where $\sigma = \pi b^2 = \pi r_c^2 v_c^2 / v_0^2 (1 - 2G_N M_{\text{NS}} / r_c)^{-1}$ is the scattering cross section for the axion star with a virial velocity v_0 approaching the neutron star with an impact parameter b . The number of axion stars is given by $n_{\text{AS}} = \kappa_{\text{AS}} \rho_{\text{DM}} / M_a \approx \kappa_{\text{AS}} \times 10^{11} \text{ pc}^{-3}$, with the galactic DM density $\rho_{\text{DM}} \sim 0.3 \text{ GeV} \cdot \text{cm}^{-3}$, while κ_{AS} is the fraction of the total DM density in dense axion stars, and f_{NS} represents the ratio of neutron stars with magnetic fields larger than 10^{13} G . We thus have $N/\text{year} = 10^{-2} \kappa_{\text{AS}} f_{\text{NS}}$ in our galaxy. The event rate per day in the Universe is $10^{13} \kappa_{\text{AS}} f_{\text{NS}} / 365 \sim 1000$, if we take conservative values of $\kappa_{\text{AS}} = 10^{-2}$ [14, 15] and $f_{\text{NS}} = 10^{-5}$ [52]. This scenario satisfies the condition that the events should be sufficiently rare to ensure that the Galactic plane does not dominate the spatial distribution of observed events [53].

In conclusion, we have proposed a new explanation for the origin of FRBs, based on the axion-to-photon conversion that ensues when a dense axion star moves through the resonant region in the pulsar magnetosphere. The observed FRB energy output is naturally obtained for axion stars with masses around $10^{-13} M_{\odot}$ if the axion-photon conversion proceeds through the non-adiabatic resonant regime. Most of the observed frequencies for non-repeating FRBs can be accommodated with a $10 \mu\text{eV}$ axion mass.

In the future, the unprecedented sensitivity of SKA and other radio telescopes may unravel the spectral properties of FRBs. The many observed events in the 0.7 to 2.1 GHz range correspond to the same intrinsic peak frequency at the emission time, which could provide further support for this scenario. Together with laboratory measurements from axion haloscopes and weak radio signals from diffuse axion DM, SKA is expected to observe many more FRBs, and might allow to pin down the correlation between FRBs, axions and DM.

We are grateful to Shmuel Nussinov for enlightening discussions and critical comments, Raymond Co,

Jonathan Katz, Oriol Pujolàs and Yicong Sui for useful discussions, Yurong Zhao for the manga. The work of JB, BD and FF is supported in part by the U.S. Department of Energy under Grant No. DE-SC0017987. FPH is supported by the McDonnell Center for the Space Sciences.

* buckley@wustl.edu

† bdev@wustl.edu

‡ ferrer@wustl.edu

§ fapeng.huang@wustl.edu (corresponding author)

- [1] R. D. Peccei and H. R. Quinn, Phys. Rev. Lett. **38**, 1440 (1977), [,328(1977)]; S. Weinberg, Phys. Rev. Lett. **40**, 223 (1978); F. Wilczek, Phys. Rev. Lett. **40**, 279 (1978); J. E. Kim, Phys. Rev. Lett. **43**, 103 (1979); M. A. Shifman, A. I. Vainshtein, and V. I. Zakharov, Nucl. Phys. **B166**, 493 (1980); M. Dine, W. Fischler, and M. Srednicki, Phys. Lett. **104B**, 199 (1981); A. R. Zhitnitsky, Sov. J. Nucl. Phys. **31**, 260 (1980), [Yad. Fiz.31,497(1980)].
- [2] P. Svrcek and E. Witten, JHEP **06**, 051 (2006), arXiv:hep-th/0605206 [hep-th]; A. Arvanitaki, S. Dimopoulos, S. Dubovsky, N. Kaloper, and J. March-Russell, Phys. Rev. **D81**, 123530 (2010), arXiv:0905.4720 [hep-th]; M. Cicoli, M. Goodsell, and A. Ringwald, JHEP **10**, 146 (2012), arXiv:1206.0819 [hep-th].
- [3] J. Preskill, M. B. Wise, and F. Wilczek, Phys. Lett. **120B**, 127 (1983); L. F. Abbott and P. Sikivie, Phys. Lett. **120B**, 133 (1983); M. Dine and W. Fischler, Phys. Lett. **120B**, 137 (1983).
- [4] I. G. Irastorza and J. Redondo, Prog. Part. Nucl. Phys. **102**, 89 (2018), arXiv:1801.08127 [hep-ph].
- [5] H. Primakoff, Phys. Rev. **81**, 899 (1951).
- [6] A. Caputo, C. P. Garay, and S. J. Witte, Phys. Rev. **D98**, 083024 (2018), [Erratum: Phys. Rev.D99,no.8,089901(2019)], arXiv:1805.08780 [astro-ph.CO]; A. Caputo, M. Regis, M. Taoso, and S. J. Witte, JCAP **1903**, 027 (2019), arXiv:1811.08436 [hep-ph].
- [7] M. S. Pshirkov and S. B. Popov, J. Exp. Theor. Phys. **108**, 384 (2009), arXiv:0711.1264 [astro-ph].
- [8] F. P. Huang, K. Kadota, T. Sekiguchi, and H. Tashiro, Phys. Rev. **D97**, 123001 (2018), arXiv:1803.08230 [hep-ph].
- [9] A. Hook, Y. Kahn, B. R. Safdi, and Z. Sun, Phys. Rev. Lett. **121**, 241102 (2018), arXiv:1804.03145 [hep-ph].
- [10] C. J. Hogan and M. J. Rees, Phys. Lett. **B205**, 228 (1988); E. W. Kolb and I. I. Tkachev, Phys. Rev. Lett. **71**, 3051 (1993), arXiv:hep-ph/9303313 [hep-ph]; Phys. Rev. **D49**, 5040 (1994), arXiv:astro-ph/9311037 [astro-ph].
- [11] D. J. Kaup, Phys. Rev. **172**, 1331 (1968); R. Ruffini and S. Bonazzola, Phys. Rev. **187**, 1767 (1969).
- [12] B. Eggemeier, J. Redondo, K. Dolag, J. C. Niemeyer, and A. Vaquero, (2019), arXiv:1911.09417 [astro-ph.CO].
- [13] E. Braaten and H. Zhang, Rev. Mod. Phys. **91**, 041002 (2019).
- [14] M. Fairbairn, D. J. E. Marsh, and J. Quevillon, Phys. Rev. Lett. **119**, 021101 (2017), arXiv:1701.04787 [astro-ph.CO].

- [15] A. Katz, J. Kopp, S. Sibiryakov, and W. Xue, JCAP **1812**, 005 (2018), arXiv:1807.11495 [astro-ph.CO].
- [16] L. Dai and J. Miralda-Escudé, Astron. J. **159**, 49 (2020), arXiv:1908.01773 [astro-ph.CO].
- [17] D. Lorimer, M. Bailes, M. McLaughlin, D. Narkevic, and F. Crawford, Science **318**, 777 (2007), arXiv:0709.4301 [astro-ph].
- [18] D. Thornton *et al.*, Science **341**, 53 (2013), arXiv:1307.1628 [astro-ph.HE].
- [19] A. Iwazaki, Phys. Rev. **D91**, 023008 (2015), arXiv:1410.4323 [hep-ph].
- [20] S. Raby, Phys. Rev. **D94**, 103004 (2016), arXiv:1609.01694 [hep-ph].
- [21] M. S. Pshirkov, Int. J. Mod. Phys. **D26**, 1750068 (2017), arXiv:1609.09658 [astro-ph.HE].
- [22] Y. Bai and Y. Hamada, Phys. Lett. **B781**, 187 (2018), arXiv:1709.10516 [astro-ph.HE].
- [23] S. B. Popov, K. A. Postnov, and M. S. Pshirkov, Phys. Usp. **61**, 965 (2018), arXiv:1806.03628 [astro-ph.HE]; J. Ye, K. Wang, and Y.-F. Cai, Eur. Phys. J. **C77**, 720 (2017), arXiv:1705.10956 [astro-ph.HE]; C.-M. Deng, Y. Cai, X.-F. Wu, and E.-W. Liang, Phys. Rev. **D98**, 123016 (2018), arXiv:1812.00113 [astro-ph.HE]; S. Sun and Y.-L. Zhang, (2020), arXiv:2003.10527 [hep-ph].
- [24] I. I. Tkachev, JETP Lett. **101**, 1 (2015), [Pisma Zh. Eksp. Teor. Fiz.101,no.1,3(2015)], arXiv:1411.3900 [astro-ph.HE].
- [25] J. G. Rosa and T. W. Kephart, Phys. Rev. Lett. **120**, 231102 (2018), arXiv:1709.06581 [gr-qc].
- [26] J. I. Katz, MNRAS **494**, L64 (2020), arXiv:1912.00526 [astro-ph.HE].
- [27] E. Petroff, E. D. Barr, A. Jameson, E. F. Keane, M. Bailes, M. Kramer, V. Morello, D. Tabbara, and W. van Straten, Publ. Astron. Soc. Austral. **33**, e045 (2016), arXiv:1601.03547 [astro-ph.HE].
- [28] <http://www.frbcat.org/>.
- [29] P. H. Chavanis and L. Delfini, Phys. Rev. **D84**, 043532 (2011), arXiv:1103.2054 [astro-ph.CO].
- [30] E. Braaten, A. Mohapatra, and H. Zhang, Phys. Rev. Lett. **117**, 121801 (2016), arXiv:1512.00108 [hep-ph].
- [31] L. Visinelli, S. Baum, J. Redondo, K. Freese, and F. Wilczek, Phys. Lett. **B777**, 64 (2018), arXiv:1710.08910 [astro-ph.CO].
- [32] P.-H. Chavanis, Phys. Rev. **D98**, 023009 (2018), arXiv:1710.06268 [gr-qc].
- [33] E. D. Schiappacasse and M. P. Hertzberg, JCAP **1801**, 037 (2018), [Erratum: JCAP1803,no.03,E01(2018)], arXiv:1710.04729 [hep-ph].
- [34] J. Eby, M. Leembruggen, L. Street, P. Suranyi, and L. C. R. Wijewardhana, Phys. Rev. **D100**, 063002 (2019), arXiv:1905.00981 [hep-ph].
- [35] I. L. Bogolyubsky and V. G. Makhankov, Pisma Zh. Eksp. Teor. Fiz. **24**, 15 (1976); M. Gleiser, Phys. Rev. **D49**, 2978 (1994), arXiv:hep-ph/9308279 [hep-ph]; M. Gleiser and A. Sornborger, Phys. Rev. **E62**, 1368 (2000), arXiv:patt-sol/9909002 [patt-sol]; G. Fodor, P. Forgacs, P. Grandclement, and I. Racz, Phys. Rev. **D74**, 124003 (2006), arXiv:hep-th/0609023 [hep-th]; P. Salmi and M. Hindmarsh, Phys. Rev. **D85**, 085033 (2012), arXiv:1201.1934 [hep-th].
- [36] J. Ollé, O. Pujolàs, and F. Rompineve, JCAP **2002**, 006 (2020), arXiv:1906.06352 [hep-ph].
- [37] T. Helfer, D. J. E. Marsh, K. Clough, M. Fairbairn, E. A. Lim, and R. Becerril, JCAP **1703**, 055 (2017), arXiv:1609.04724 [astro-ph.CO].
- [38] A. Arvanitaki, S. Dimopoulos, M. Galanis, L. Lehner, J. O. Thompson, and K. Van Tilburg, (2019), arXiv:1909.11665 [astro-ph.CO].
- [39] B. Garbrecht and J. I. McDonald, JCAP **1807**, 044 (2018), arXiv:1804.04224 [astro-ph.CO].
- [40] L. Spitler *et al.*, Nature **531**, 202 (2016), arXiv:1603.00581 [astro-ph.HE].
- [41] B. Andersen *et al.* (CHIME/FRB), Astrophys. J. Lett. **885**, L24 (2019), arXiv:1908.03507 [astro-ph.HE].
- [42] Amiri *et al.* (CHIME/FRB), (2020), arXiv:2001.10275 [astro-ph.HE].
- [43] C. Hagmann, P. Sikivie, N. S. Sullivan, and D. B. Tanner, Phys. Rev. **D42**, 1297 (1990).
- [44] M. Tanabashi *et al.* (Particle Data Group), Phys. Rev. **D98**, 030001 (2018).
- [45] G. G. Raffelt, *Stars as laboratories for fundamental physics* (1996).
- [46] P. Goldreich and W. H. Julian, Astrophys. J. **157**, 869 (1969).
- [47] F. Weber, *Pulsars as astrophysical laboratories for nuclear and particle physics* (1999).
- [48] G. Raffelt and L. Stodolsky, Phys. Rev. D **37**, 1237 (1988).
- [49] E. Petroff, J. W. T. Hessels, and D. R. Lorimer, Astron. Astrophys. Rev. **27**, 4 (2019), arXiv:1904.07947 [astro-ph.HE].
- [50] A. Payez, J. R. Cudell, and D. Hutsemekers, AIP Conf. Proc. **1241**, 444 (2010), arXiv:0911.3145 [astro-ph.CO]; Phys. Rev. D **84**, 085029 (2011), arXiv:1107.2013 [astro-ph.CO]; D. Horns, L. Maccione, A. Mirizzi, and M. Roncadelli, Phys. Rev. D **85**, 085021 (2012), arXiv:1203.2184 [astro-ph.HE]; E. Masaki, A. Aoki, and J. Soda, Phys. Rev. D **96**, 043519 (2017), arXiv:1702.08843 [astro-ph.CO].
- [51] D. J. Bacon *et al.* (SKA), Submitted to: Publ. Astron. Soc. Austral. (2018), arXiv:1811.02743 [astro-ph.CO].
- [52] P. Beniamini, K. Hotokezaka, A. van der Horst, and C. Kouveliotou, Mon. Not. Roy. Astron. Soc. **487**, 1426 (2019), arXiv:1903.06718 [astro-ph.HE].
- [53] J. I. Katz, Prog. Part. Nucl. Phys. **103**, 1 (2018), arXiv:1804.09092 [astro-ph.HE].